JOURNAL OF GEOPHYSICAL RESEARCH, VOL. 114, F01029, doi:10.1029/2008JF000981, 2009

A nonlocal theory of sediment buffering and bedrock channel evolution

Colin P. Stark,[1] Efi Foufoula-Georgiou,[2] and Vamsi Ganti[2]

Received 8 January 2008; revised 2 June 2008; accepted 11 September 2008; published 7 March 2009.

[1] Bedrock erosion in mountain river channels ultimately sets the erosion rate of the surrounding hillslopes and the rate of sediment supply to the channels. The supply of coarse bed sediment acts as a dampening effect on further erosion by depositing an alluvial cover that temporarily obscures the bedrock. For landscapes where the residence time of the alluvial bed cover is comparable to the timescale of bedrock incision, coarse sediment supply and transport generate a strong negative feedback on fluvial downcutting and the coupled process of hillslope-channel erosion is inherently self-buffering. Here we study a simple model of self-buffered bedrock channel erosion that incorporates the spreading of bed sediment cover downstream in a way that allows for a broad-tailed, power law probability distribution of transport velocities of bed sediment over the long-term. This leads us to consider a nonlocal transport law (fractional advection) parameterized by a scaling exponent $0 \leq \alpha < 1$ which collapses to local advection for $\alpha \rightarrow 1$. For strong sediment buffering, we find that nonlocality $1 - \alpha$ has a direct control on the power law scaling of channel slope S with upstream area A, giving $S \sim A^{-(1-\alpha)/2}$ at steady state. Empirical observations of slope-area scaling are consistent with $\alpha < 1$ and nonlocal transport. In general, the model predicts linear, logarithmic, or power law stream profiles depending on the extent of buffering, the degree of nonlocality, and the scaling of the bedrock erosion law. It also predicts, somewhat counterintuitively, that bed cover should thicken with distance x downstream slower than linearly as x^{α}, i.e., the more nonlocal the bed sediment spreading process ($\alpha \rightarrow 0$), the slower the bed cover increases downstream. We deduce that long-range, heterogeneous transport of coarse sediment in mixed bedrock-alluvial rivers may be a key element of landscape scaling and an important factor in landscape dynamics.

Citation: Stark, C. P., E. Foufoula-Georgiou, and V. Ganti (2009), A nonlocal theory of sediment buffering and bedrock channel evolution, *J. Geophys. Res.*, *114*, F01029, doi:10.1029/2008JF000981.

1. Introduction

[2] Mountain river channels with naked bedrock beds are rare [*Tinkler and Wohl*, 1998]. Most have an alluvial cover of coarse, bedload-grade sediments; this cover can be meters to tens of meters thick or more and can persist for thousands of years after deposition before the bedrock is exposed once again to erosion [*Turowski et al.*, 2008] (the more appropriate term for most "bedrock rivers" should be "mixed bedrock-alluvial rivers"). Nevertheless, most of the theoretical treatment of mountain river erosion has focused on true bedrock channels [*Dietrich et al.*, 2003; *Stock and Montgomery*, 1999; *Snyder et al.*, 2003; *Whipple and Tucker*, 1999; *Whipple*, 2004; *Tucker and Bras*, 2000; *Sklar and Dietrich*, 1998, 2001; *Stark*, 2006; *Wobus et al.*, 2006] and the role of alluvial bed cover in the buffering of channel erosion has been sparsely studied [e.g., *Finnegan et al.*, 2007; *Sklar and Dietrich*, 2004, 2006].

[3] Alluvial bed cover develops through the coupled processes of hillslope erosion, channel incision and channel transport. Broadly speaking, hillslope erosion is slave to channel erosion (particularly on long timescales) with the average rate of catchment denudation essentially driven by the rate of downcutting in the channels. The greater the downcutting rate, the greater the flux of sediment into the channels, and therefore the greater the likely temporary storage of bedload-grade sediment along the channels.

[4] A continuum description of this kind understates the problem: on the short-term or storm event timescale, the patterns and rates of sediment supply and transport are strongly heterogeneous, and the transient nature of bed sediment storage is more pronounced. Mass-wasting events supplying coarse material to the channels often occur asynchronously to the high-stage flows capable of transporting such material [*Dadson*, 2004; *Gabet et al.*, 2008]; the volume of mass-wasted material may require hundreds to thousands or more flood events to completely flux the coarse sediment through the drainage network; the asynchroneity is exacerbated when

[1] Lamont-Doherty Earth Observatory, Columbia University, Palisades, New York, USA.
[2] St. Anthony Falls Laboratory, University of Minnesota, Minneapolis, Minnesota, USA.

0148-0227/09/2008JF000981$09.00

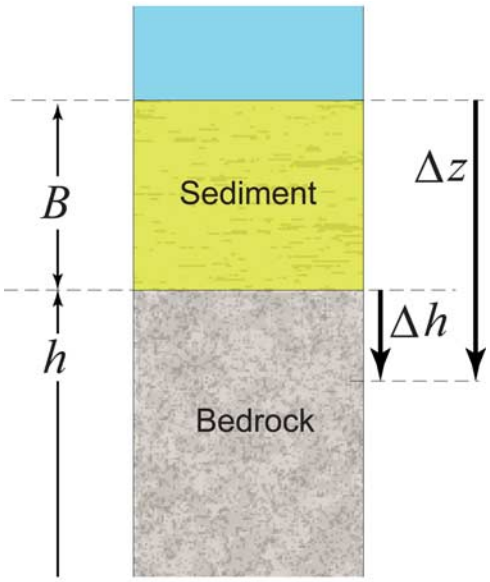

Figure 1. Schematic erosion of bed sediment cover and bedrock.

the mass-wasting events are triggered by earthquakes that deliver sediment independently of the storm events that generate the river flows capable of significant bed sediment transport [e.g., *Dadson et al.*, 2004; *Harp and Jibson*, 1996]; earthquake-driven mass wasting can saturate mountain river channels with coarse debris for very long periods of time, both by immediately generating landslides and debris flows and by priming the hillslopes for widespread failure during later heavy rainfall events [e.g., *Lin et al.*, 2003].

[5] Therefore, while bedrock incision in mountain rivers drives erosion of the surrounding hillslopes, it also impedes further incision by drawing coarse hillslope sediment onto the channel bed. This self-limiting, negative feedback process can be thought of as "sediment buffering." The purpose of this paper is to present a simple model for mountain river erosion that incorporates sediment buffering, i.e., a model to describe the evolution of a mixed bedrock-alluvial channel in which bed sediment cover may be the rate-limiting factor.

[6] The model addresses a second key issue in mountain rivers whose importance becomes clear when attempting to treat the heterogeneous transport of bed sediment through a catchment: the long-term motion of coarse sediment particles is not a spatially limited process that can be estimated by computing local bedload motions at each channel cross section. In reality, grains of bed sediment of variable mass are transported with a broad range of particle velocities over a wide range of distances by numerous flood discharges of varying magnitude [*Stark et al.*, 2000]. Although the composite, long-term probability distribution of transport distances is not yet known empirically, studies such as those of *Hassan and Church* [1991] and *Church and Hassan* [1992] have recorded semiheavy (exponential or gamma) probability density functions (pdfs) of particle transport distances after one or two floods, and on theoretical grounds it is reasonable to deduce that it is heavy tailed. Probability distributions with heavy, power law tails arise in nature for one of (at least) three reasons: (1) because the governing process is self-similar, (2) through the mixing of distributions of constituent properties (Appendix A2), or (3) through summation of quantities with arbitary shape, broad-tailed distributions and convergence to a stable law pdf according to the Lévy limit theorem [*Lévy*, 1937; *Feller*, 1971]. All three phenomena are likely to pertain to the distributions of bed particle motions in mixed bedrock-alluvial rivers.

[7] The implication of a power-law tail is that the bed sediment acting to buffer bedrock erosion is spread from its hillslope supply points in a way that deviates from a simple advection process. Instead, the spreading process is probably strongly heterogenous, nonclassical, and best described using a fractional advection model [e.g., *Baeumer et al.*, 2001]. This heterogeneity needs to be incorporated in models of mixed bedrock-alluvial channel evolution, because its long-range properties will significantly affect the pattern of sediment distribution across the catchment and may ultimately determine the scaling relationships between channel gradient and upstream area.

2. Principles

[8] There are two key elements to the model: (1) the coupled process of bed sediment buffering and bedrock erosion and (2) the nonlocal spreading downstream of bed sediment. There are two key innovations that make the model tractable: (1) the conceit that the erosion of both sediment and bedrock can be treated in a consistent manner by writing the rates of both in terms of unit stream power and (2) the application of fractional calculus to the description of nonlocal advection of bed sediment.

[9] The governing equations are derived in detail in section 3 and are summarized here to stress the explicit coupling of the bed cover thickness and the temporal evolution of the channel profile. The rate of bedrock channel incision is given by

$$-\frac{\partial h}{\partial t} \sim \eta_{\text{rock}}\left(\frac{\Omega}{x} - \frac{B}{\eta_{\text{sed}}}\right), \tag{1}$$

where h is the elevation of channel bedrock profile (subject here to zero rock uplift rate), Ω is unit stream power, x is downstream distance (here implicitly giving channel width scale), t is time, $B(x, t)$ is the bed cover thickness, and η_{rock} and η_{sed} are bedrock and sediment erodibilities, respectively. The downstream spreading of coarse bed sediment is

$$x\frac{\partial B}{\partial t} \sim -v_0\frac{\partial}{\partial x}\left(x^2 I_x^{1-\alpha}\left\{\frac{B}{x}\right\}\right) - x\frac{\partial h}{\partial t} \tag{2}$$

where v_0 is a reference transport speed of bed sediment and $1 - \alpha$ is the degree of nonlocality of this transport (spreading) process, specifically, α is the exponent in the heavy-tailed probability distribution of transport velocities $p(v)$ that is encapsulated in the fractional integral $I_x^{1-\alpha}\{\cdot\}$.

3. Theory

3.1. Bed Cover Buffering

[10] Consider the time interval $\Delta\tau$ over which the bed sediment cover of thickness B is "eroded," the bedrock bed is exposed, and then the bedrock itself is eroded (Figure 1)

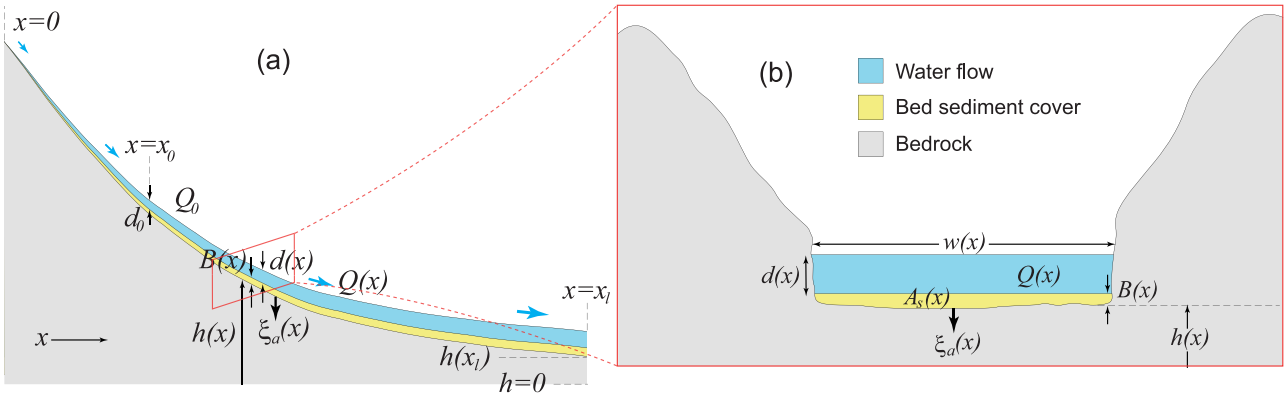

Figure 2. Model geometry shown in (a) downstream profile and (b) cross section.

by $-\Delta h \geq 0$ (h is measured positive upward); the net bedrock erosion during $\Delta\tau$ is therefore $\Delta z = B - \Delta h$. Define λ as the fraction of time spent in eroding sediment and ξ_{raw} as the raw (unscaled by material erodibilities) rate of erosion. The time spent eroding the bedrock is

$$(1-\lambda)\Delta\tau = \frac{-\Delta h}{\eta_{\text{rock}}\xi_{\text{raw}}} \tag{3}$$

and the time spent "eroding" the sediment is

$$\lambda\Delta\tau = \frac{B}{\eta_{\text{sed}}\xi_{\text{raw}}}, \tag{4}$$

so that

$$\Delta\tau = \left(\frac{-\Delta h}{\eta_{\text{rock}}} + \frac{B}{\eta_{\text{sed}}}\right)\frac{1}{\xi_{\text{raw}}}, \tag{5}$$

where η_{rock} and η_{sed} are the respective erodibilities of rock and bed sediment. Rearranging, we obtain the actual bedrock erosion rate ξ_{a}

$$-\frac{\Delta h}{\Delta\tau} \rightarrow -\partial_t h = \xi_a = \eta_{\text{rock}}\xi_{\text{raw}} - \frac{\eta_{\text{rock}}}{\eta_{\text{sed}}}\frac{B}{\Delta\tau}. \tag{6}$$

If the bedrock is undergoing vertical motion, the frame of reference for h is moving and the rate of lowering of the profile $-\partial_t h$ must also include a term giving the rate of uplift (see below).

3.2. Dimensionless Bed Cover

[11] The cross-sectional area of the channel (Figure 2) taken up by bed sediment is

$$A_s(x,t) = wB(x,t) = wdC(x,t), \tag{7}$$

where w and d are the width and depth of the channel and B is the bed cover thickness, which can be expressed in terms of the dimensionless bed cover C as

$$B(x,t) = dC. \tag{8}$$

The parameter $C(x, t)$ is effectively the fraction of channel cross-sectional area occupied by bed sediment, so it can be thought of (loosely) as a sediment concentration in the flow at the channel cross section at a distance downstream x.

3.3. Nonlocal Bed Sediment Transport

[12] If grains of sediment pass through a channel cross-section x with a constant velocity (or random velocities following a probability distribution with a light tail), then $C(x, t)$ can be approximated by the number of particles in a thin strip of downstream width Δx. However, if the particle velocities follow a distribution with a heavy tail then the narrow strip Δx is too small to statistically capture particles that originate from far away transported at great speed. Thus one needs to enlarge the width of the strip to accommodate the heavy-tailed pdf of velocities.

[13] This is equivalent to saying that instead of considering a local flux $\phi(x)$ determined by the local particle concentration and velocities, one should consider a nonlocal, compound flux

$$\phi^*(x,t) = \int_0^x g(l)\phi(x-l,t)\mathrm{d}l, \tag{9}$$

where the weighting function $g(l)$ should account for the likelihood of an incoming particle arriving from a distance l upstream of a location x. For a velocity distribution with a power law tail with exponent α (Appendix A2)

$$\mathbb{P}(V \geq v) \sim v^{-\alpha} \qquad 0 \leq \alpha < 1 \tag{10}$$

the weights take the form of a power law on lag

$$g(l) \sim l^{-\alpha} \tag{11}$$

and the nonlocal flux (volume per unit channel cross-sectional area per unit time) is equivalent (Appendix A1) to the fractionally integrated flux

$$\phi^*(x,t) = \frac{v_0}{x_0^{1-\alpha}} I_x^{1-\alpha}\{C(x,t)\}, \tag{12}$$

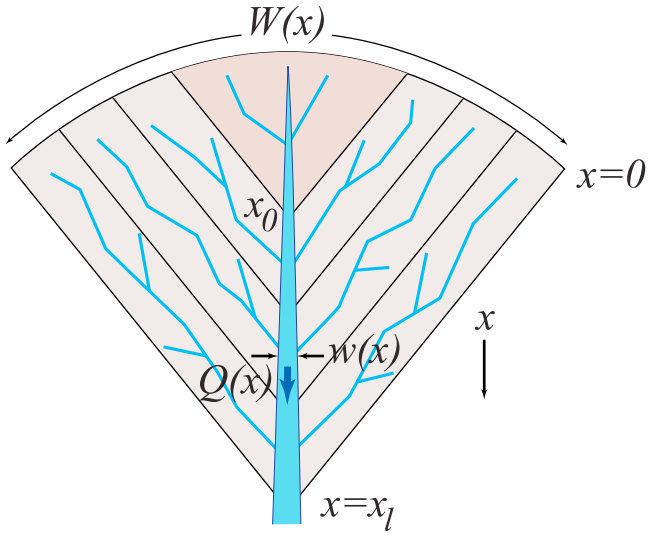

Figure 3. Nested catchment geometry used in model. The drainage network shown here is schematic.

where v_0 is a reference speed. It is worth noting that if we take the limit as $\alpha \to 1$ we recover the local flux $\phi(x, t)$ (simple advection). The corresponding sediment discharge (volume per unit time) through a channel cross section of mean flow width w and depth d at a distance x downstream is

$$Q_s(x,t) = wd\phi^*. \tag{13}$$

[14] A heavy-tailed distribution of bed particle velocities (equation (10)) is used here to model (without distinction) both a power law pdf of velocities during a single flood and a power law pdf of particle transport distances over multiple floods and a long timescale. Such a heavy-tailed pdf is likely given the heterogeneous, composite nature of the stochastic process of sediment transport in mountain rivers, and given the ease with which heavy-tailed pdfs can arise through the mixing of lighter tailed pdfs (see Appendix A2 for an example of the mixing of exponential and gamma distributions of grain size and transport distance to give a composite particle velocity pdf with a power law tail).

3.4. Bedrock Erosion Model

[15] To make the linkage in a simple way between stream flow, stream power, bedrock erosion, raw bedrock channel incision, sediment-buffered channel incision and ultimately the channel slope-upstream-area relation, we assume here a linear model of channel bedrock erosion as a function of unit stream power per unit channel width w. The unit stream power at the characteristic flood discharge Q is

$$\Omega(Q) = \rho g Q|\partial_x h|, \tag{14}$$

whose units are W/m or energy dissipated per unit time per unit distance downstream [*Rhoads*, 1987]. If bedrock erosion is linearly proportional to the rate of energy dissipation per unit area Ω/w, then the amount of vertical lowering during flood events of discharge Q, duration t_f and annual frequency f, and reference bedrock erodibility γ (whose reciprocal has units of J/m^3), is

$$\xi_{\text{raw}} = f t_f \gamma \frac{\Omega}{w} = f t_f \gamma \rho g \frac{Q|\partial_x h|}{w}, \tag{15}$$

which can be simplified by defining a flood effectiveness term

$$\mu = t_f \gamma \rho g, \tag{16}$$

which has units of reciprocal velocity (seconds per meter). For downstream always-negative gradients the raw rate of erosion per year becomes

$$\xi_{\text{raw}} = f \mu \frac{Q}{w}(-\partial_x h). \tag{17}$$

The sediment-buffered, actual rate of bedrock erosion, for bedrock with erodibility $\eta_r = \eta_{\text{rock}}$ and sediment cover with erodibility $\eta_s = \eta_{\text{sed}}$ comes from combining equation (6) with equation (17), and assuming $f = 1/\Delta\tau$,

$$\xi_a = f \eta_r \left(\mu \frac{Q}{w}(-\partial_x h) - \frac{1}{\eta_s} B \right). \tag{18}$$

This is our first governing equation.

3.5. Sediment Supply

[16] Sediment supply from coupled erosion of the main channel, its tributaries and all surrounding hillslopes yields a total input of coarse sediment per unit downstream distance of

$$\varphi(x,t) = \chi \frac{\mathrm{d}A_c}{\mathrm{d}x} \xi_a = \chi W \xi_a, \tag{19}$$

where $A_c(x)$ is the catchment area and $W(x)$ is an effective catchment width (Figure 3). The prefactor χ is the coarse fraction of eroded material that becomes bed sediment in our model; the remaining proportion of sediment is assumed to be suspended or wash load.

3.6. Mass Balance

[17] Conservation of nonlocal bed sediment flux (equation (13)) gives

$$\partial_t A_s = -\partial_x Q_s + \varphi = -\partial_x \{wd\phi^*\} + \chi W \xi_a, \tag{20}$$

where $\partial_x\{\cdot\}$ is the divergence operator and A_s is the bed-sediment cross-sectional area (Figure 2b). This is our second governing equation.

[18] As a cross-check, lets see what would happen if there were no fractional advection and no source term

$$\partial_t \{x^2 C\} = -v_0 \partial_x \{x^2 C\}, \tag{21}$$

which simplifies to

$$\mathcal{D}\{A_s\} = \partial_t A_s + v_0 \partial_x A_s = 0, \tag{22}$$

which means that in the Lagrangian frame of the flow of sediment moving at speed v_0 downstream, the cross-sectional volume per unit distance downstream A_s is constant.

3.7. Rock Uplift Rate

[19] The vertical reference frame is set by the pattern of relative base level change ("uplift") $u(x, t)$ so that the absolute elevation of the river profile bedrock base is

$$\partial_t h = u(x,t) - \xi_a. \tag{23}$$

For the remainder of this paper we will assume a uniform and constant uplift rate $u(x, t) = u_0$ over the domain $0 \leq x \leq x_l$.

4. Implementation

[20] The model is implemented in an idealized catchment geometry with simple hydraulic geometry and scaling (Figures 2 and 3).

4.1. Hydraulic Geometry

[21] The characteristic flood discharge $Q(x)$ is assumed for simplicity to scale linearly with drainage area

$$Q(x) = Q_0\left(\frac{x}{x_0}\right)^2. \tag{24}$$

Noninteger scaling (Hack's law) could be employed here if required. Uniformly constant downstream flow speed is assumed, along with a roughly rectangular channel cross section, an implicit Chézy formulation of steady open channel flow resistance and consequent hydraulic geometry, which means that the flow width (Figure 2b) scales as root discharge

$$w(Q(x)) = w_0\sqrt{\frac{Q(x)}{Q_0}} = w_0\sqrt{\frac{x^2}{x_0^2}} = \frac{w_0}{x_0}x \tag{25}$$

as does flow depth

$$d(Q(x)) = d_0\sqrt{\frac{Q(x)}{Q_0}} = d_0\sqrt{\frac{x^2}{x_0^2}} = \frac{d_0}{x_0}x. \tag{26}$$

The scaling of discharge per unit channel width is important

$$\frac{Q}{w} = \left(Q_0\left(\frac{x}{x_0}\right)^2\right)\Big/\left(\frac{w_0}{x_0}x\right) = \left(\frac{Q_0}{w_0x_0}\right)x \tag{27}$$

because it determines the scaling in the raw erosion rate calculation (equation (18)).

4.2. Catchment Geometry

[22] Catchment widening with downstream distance is the arc length for the "pie-shaped" drainage basin (Figure 3)

$$W(x) = \frac{W_0}{x_0}x. \tag{28}$$

The catchment area is the integral over x

$$A_c(x) = \frac{W_0}{2x_0}x^2. \tag{29}$$

4.3. Model Dynamics

[23] We can reduce the model equations (18) and (20) to a coupled pair of partial differential equations by incorporating the pattern of rock uplift, which in this treatment is assumed to be spatiotemporally uniform (equation (23)). The PDE pair is a closed form description of the evolution of the bedrock river profile over time and space.

[24] The constitutive equation, which describes bed-sediment buffered channel bedrock erosion ξ_a, is

$$u_0 - \partial_t h = f\eta_r x\left\{\left(\frac{\mu Q_0}{w_0x_0}\right)(-\partial_x h) - \left(\frac{d_0}{\eta_s x_0}\right)C\right\}. \tag{30}$$

The conservation equation, which describes the hillslope supply and downstream river channel spreading of bed sediment, is

$$x^2\partial_t C = -v_0\partial_x\left\{\frac{1}{x_0^{1-\alpha}}x^2 I_x^{1-\alpha}C\right\} + \left(\frac{\chi W_0x_0}{w_0d_0}\right)x(u_0 - \partial_t h). \tag{31}$$

[25] The formulation and solution of such a coupled system of fractional advection and partial differential equations (with nonlinear terms) is wholly original. To date, the focus in the literature has been on fractional dispersion [e.g., *Benson*, 1998] and where nonlocal advection has been addressed [*Baeumer et al.*, 2001; *Zhang et al.*, 2007] it has taken a different form (Appendix A3).

5. Steady State Solution

[26] If we assume that the time scale of bedrock channel evolution is large compared to the equilibration timescale of the bed sediment, $t_h \gg t_c$, then C is effectively instantly equilibrated and therefore constant at the timescale of bedrock channel evolution. This implies that

$$\partial_t\{x^2C\} = x^2\partial_t C = 0. \tag{32}$$

Erosion rates balance the mass input everywhere at steady state, so that (equation (23))

$$\xi_a = u_0 \quad \Leftrightarrow \quad -\partial_t h = 0. \tag{33}$$

From equation (31) we have

$$\partial_x\left\{\frac{1}{x_0^{1-\alpha}}x^2 I_x^{1-\alpha}C\right\} = \left(\frac{\chi W_0x_0}{v_0w_0d_0}\right)u_0x. \tag{34}$$

Integrating out gives

$$x^2 I_x^{1-\alpha}C = \left(\frac{\chi W_0x_0^{2-\alpha}}{v_0w_0d_0}\right)u_0\int_{x_{hc}}^{x}\zeta\mathrm{d}\zeta. \tag{35}$$

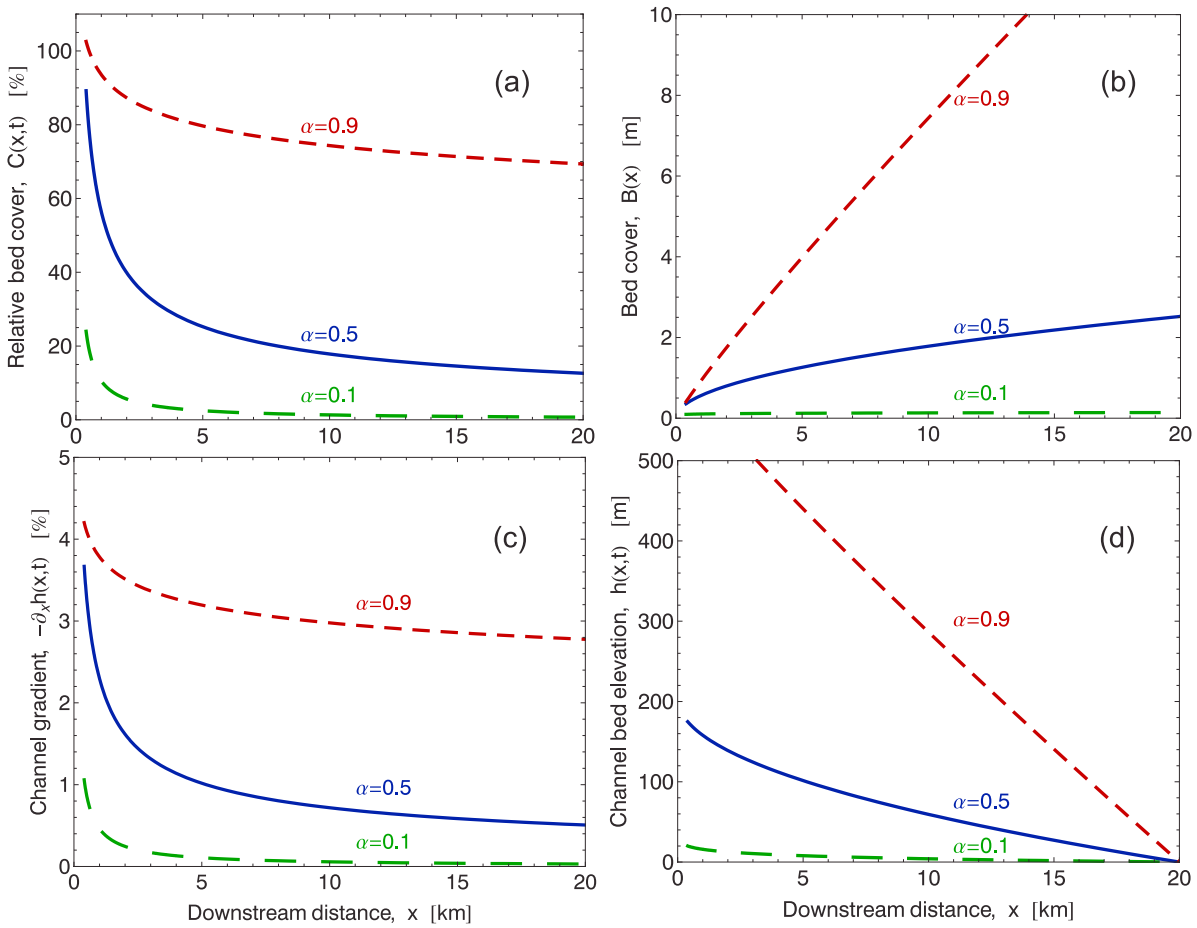

Figure 4. Steady state solutions for (a) dimensionless bed sediment cover $C(x,\ t \rightarrow \infty)$, (b) bed sediment thickness $B(x,\ t \rightarrow \infty)$, (c) channel gradient $-\partial_x h(x,\ t \rightarrow \infty)$, and (d) channel bedrock bed elevation $h(x,\ t \rightarrow \infty)$ for three models with $\alpha = 0.1$ (long-dashed line), $\alpha = 1/2$ (solid line), and $\alpha = 0.9$ (short-dashed line).

The drainage divide $x = 0$ is the lower limit of the fractional integration $I_x^{\alpha}\{\cdot\}$ (see Appendix) and x_{hc} is the hillslope-channel transition length scale. The fractional differentation and integration operations here are associative and this equation can be rearranged to give

$$C(x, t \rightarrow \infty) = \left(\frac{\chi W_0 x_0^{2-\alpha}}{v_0 w_0 d_0}\right) u_0 \partial_x^{1-\alpha}\left\{\frac{x^2 - x_{hc}^2}{2x^2}\right\}. \tag{36}$$

Since $0 \leq \alpha < 1$ this is a fractional derivative. For simplicity, we assume that the hillslope-channel transition length scale is $x_{hc} \approx 0$ so that we have

$$C(x, t \rightarrow \infty) = \frac{1}{\Gamma(\alpha)}\left(\frac{\chi W_0 x_0}{2 w_0 d_0}\right)\left(\frac{u_0}{v_0}\right)\left(\frac{x}{x_0}\right)^{\alpha - 1}. \tag{37}$$

[27] This closed form result for the dimensionless bed cover is illustrated in Figure 4a for three values of α and the example set of model parameters given in section 8. In the limit as $\alpha \rightarrow 1$, fractional integration is turned off and we recover the result derived above for the nonfractional case with $x_{hc} = 0$

$$C(x, t \rightarrow \infty) = \left(\frac{\chi W_0 x_0}{2 w_0 d_0}\right)\left(\frac{u_0}{v_0}\right). \tag{38}$$

The bed sediment thickness for any α is derived by combining equations (8), (26) and (37)

$$B(x, t \rightarrow \infty) = \frac{1}{\Gamma(\alpha)}\left(\frac{\chi W_0 x_0}{2 w_0}\right)\left(\frac{u_0}{v_0}\right)\left(\frac{x}{x_0}\right)^{\alpha}. \tag{39}$$

This result is illustrated in Figure 4b for three values of α and the example set of model parameters given in section 8.

5.1. Channel Slope

[28] Combining equations (30) and (33), we find the channel gradient at steady state can be written as

$$(-\partial_x h) = \left(\frac{w_0 x_0}{f \eta_r \mu Q_0}\right)\frac{1}{x}\left\{u_0 + f\left(\frac{\eta_r}{\eta_s}\right)\left(\frac{d_0}{x_0}\right) x C\right\}. \tag{40}$$

Substitution of the dimensionless bed cover $C(x,\ t \rightarrow \infty)$ given by equation (37) gives

$$-\partial_x h(x, t \rightarrow \infty) = \left(\frac{w_0 x_0}{f \eta_r \mu Q_0}\right)\frac{1}{x} \times \left\{u_0 + f\left(\frac{\eta_r}{\eta_s}\right)\left(\frac{d_0}{x_0}\right)\frac{1}{\Gamma(\alpha)}\left(\frac{\chi W_0 x_0^2}{2 w_0 d_0}\right)\left(\frac{u_0}{v_0}\right)\left(\frac{x}{x_0}\right)^{\alpha}\right\}, \tag{41}$$

which simplifies to

$$-\partial_x h(x, t \to \infty) = \left(\frac{w_0 x_0}{\eta_r \mu Q_0}\right)\left(\frac{u_0}{v_0}\right) \times \left\{\left(\frac{v_0 x^{-\alpha}}{f x_0^{1-\alpha}}\right) + \frac{1}{\Gamma(\alpha)}\left(\frac{\eta_r}{\eta_s}\right)\left(\frac{\chi W_0}{2w_0}\right)\right\}\left(\frac{x}{x_0}\right)^{\alpha-1}. \quad (42)$$

Several key aspects of model behavior can be gleaned from this equation. The two bracketed terms describe the respective importance of raw (left) versus buffered (right) bedrock erosion. If buffering is very weak, the right-hand bracketed term vanishes and the rate of channel bedrock incision is given simply by the raw rate of erosion (equation (15)); the channel slope has a hyperbolic decay that originates in the simple erosion law scaling:

$$-\partial_x h(x, t \to \infty) \approx \left(\frac{w_0 u_0}{f \eta_r \mu Q_0}\right)\left(\frac{x}{x_0}\right)^{-1}. \quad (43)$$

On the other hand, if buffering is strong, or if we simply examine the asymptotic limit for large x downstream, we find that channel slope is a power law decay

$$-\partial_x h(x \to \infty, t \to \infty) \approx \frac{1}{\Gamma(\alpha)}\left(\frac{\chi W_0 x_0}{2\eta_s \mu Q_0}\right)\left(\frac{u_0}{v_0}\right)\left(\frac{x}{x_0}\right)^{\alpha-1}, \quad (44)$$

with exponent $\alpha - 1$ such that the decay is bounded between x^0 and x^{-1}. In other words, at the limiting values of α, we find the model predicts a constant gradient (and a linear river profile) for purely local bed sediment transport and $\alpha = 1$, whereas it predicts a hyperbolic decay in slope (and a logarithmic river profile) for extremal nonlocal transport ($\alpha = 0$) (see Figure 4c).

5.2. Channel Elevation

[29] For the case of negligible bed buffering, integration of equation (43) with $h(x_0) = h_0$ results in the river profile

$$h(x, t \to \infty) \approx h_0\left\{1 - \left(\frac{w_0 u_0}{f \eta_r \mu Q_0}\right)\log\left(\frac{x}{x_0}\right)\right\}. \quad (45)$$

For the case of significant bed buffering, and/or for large x, integration of equation (44) results instead in the profile

$$h(x, t \to \infty) \approx h_0\left\{1 - \frac{1}{\Gamma(\alpha)}\left(\frac{\chi W_0 x_0}{2\alpha\eta_s \mu Q_0}\right)\left(\frac{u_0}{v_0}\right)\left(\frac{x}{x_0}\right)^{\alpha}\right\}. \quad (46)$$

This closed form result is illustrated in Figure 4d for three values of α and the example set of model parameters given in section 8.

5.3. Mass Balance

[30] The nonlocal sediment flux at steady state can be found by substituting the solution for dimensionless bed cover $C(x, t \to \infty)$ given by equation (37) into the fractional advection flux equation (12), which gives

$$\phi^*(x, t \to \infty) = \frac{1}{\Gamma(\alpha)}\left(\frac{\chi W_0 x_0}{2w_0 d_0}\right) u_0 I_x^{1-\alpha}\{x^{\alpha-1}\} \quad (47)$$

and thus

$$\phi^*(x, t \to \infty) = \left(\frac{\chi W_0 x_0}{2w_0 d_0}\right) u_0. \quad (48)$$

The sediment discharge is then

$$Q_s(x, t \to \infty) = w d \phi^* = \left(\frac{w_0 d_0}{x_0^2}\right)\left(\frac{\chi W_0 x_0}{2w_0 d_0}\right) u_0 x^2 \quad (49)$$

and thus

$$Q_s(x, t \to \infty) = \left(\frac{\chi W_0}{2x_0}\right) u_0 x^2, \quad (50)$$

which is consistent with simple mass balance, since this gives

$$Q_s(x, t \to \infty) = \chi A_c u_0. \quad (51)$$

Alternatively, we can integrate out the divergence in the second PDE,

$$\partial_x Q_s = \varphi(x), \quad (52)$$

so that using equation (19) yields

$$Q_s(x, t \to \infty) = \left(\frac{\chi W_0}{x_0}\right) u_0 \int_0^x \zeta \mathrm{d}\zeta, \quad (53)$$

which gives the same result.

5.4. Slope-Area Scaling

[31] A key result of our model is the scaling of slope

$$S = -\partial_x h, \quad (54)$$

with area

$$A = A_c = \frac{W_0}{2x_0} x^2, \quad (55)$$

which we find is

$$S \sim A^{-(1-\alpha)/2}. \quad (56)$$

In other words, the scaling exponent in the standard form of this equation

$$S \sim A^{-\theta} \quad (57)$$

is

$$\theta = \frac{1-\alpha}{2}. \quad (58)$$

[32] The implication is that if sediment buffering by fractional advection (in the simple scaling form presented here) were the only control on slope-area scaling, slopes would decrease no faster than $A^{-1/2}$

$$0 \le \alpha < 1 \quad \Leftrightarrow \quad \frac{1}{2} \ge \theta > 0. \quad (59)$$

Empirical studies of slope-area scaling [e.g., *Gupta and Waymire*, 1989; *Tarboton et al.*, 1989; *Sklar and Dietrich*, 1998; *Whipple*, 2004] typically find exponents around 1/2 or higher, which indicates that (1) advection is likely strongly nonlocal and (2) some of our model scaling simplifications, particularly in the treatment of hydraulic geometry, will need to be reexamined in future model developments to allow $\theta > 1/2$. Nevertheless, the main conclusion to draw is that our sediment buffering model offers an alternative explanation to the standard interpretation of slope-area power law scaling originating in a stream power law for bedrock erosion rate [e.g., *Montgomery*, 2001; *Whipple and Tucker*, 1999].

6. Time-Dependent Behavior

[33] The trick of assuming that C instantly adjusts to prevailing conditions on timescales $t_h \gg t_c$ can be extended to allow solution of the time-dependent behavior of bedrock channel evolution $h(x, t)$. In the conservation equation (31), the dimensionless sediment cover is effectively constant over time, so that the sediment cross-sectional area is also constant

$$\partial_t A_s = 0 \tag{60}$$

in equation (20). Thus the sediment discharge increases only over space (downstream) and not time by the sediment supply function

$$\partial_x Q_s = \varphi(x), \tag{61}$$

which expands, using equations (19), (23), and (28), into

$$\partial_x Q_s = \left(\frac{\chi W_0}{x_0}\right)(u_0 - \partial_t h)x. \tag{62}$$

In terms of the sediment flux, this equation can be written using equation (13) as

$$\partial_x\{wd\phi^*\} = \left(\frac{\chi W_0}{x_0}\right)(u_0 - \partial_t h)x, \tag{63}$$

which expands, using equations (25) and (26), to

$$\partial_x\left\{\frac{w_0 d_0}{x_0^2}x^2\phi^*\right\} = \left(\frac{\chi W_0}{x_0}\right)(u_0 - \partial_t h)x, \tag{64}$$

and then using equation (12) to

$$v_0\left(\frac{w_0 d_0}{x_0^{3-\alpha}}\right)\partial_x\{x^2 I_x^{1-\alpha}C\} = \left(\frac{\chi W_0}{x_0}\right)(u_0 - \partial_t h)x \tag{65}$$

or

$$v_0\partial_x\left\{\frac{1}{x_0^{1-\alpha}}x^2 I_x^{1-\alpha}C\right\} = \left(\frac{\chi W_0 x_0}{w_0 d_0}\right)(u_0 - \partial_t h)x. \tag{66}$$

Integrating out we obtain

$$\frac{v_0}{x_0^{1-\alpha}}x^2 I_x^{1-\alpha}C = \left(\frac{\chi W_0 x_0}{w_0 d_0}\right)\int_0^x (u_0 - \partial_t h)\zeta \mathrm{d}\zeta, \tag{67}$$

which is a useful form for numerical solution (section 7). It is always true that

$$C = \partial_x^{1-\alpha}\{I_x^{1-\alpha}C\}, \tag{68}$$

which allows rearrangement of equation (67) to give the dimensionless sediment cover in an explicit form

$$C(x, t \gg t_c) = \left(\frac{x_0^{1-\alpha}}{v_0}\right)\left(\frac{\chi W_0 x_0}{w_0 d_0}\right)\partial_x^{1-\alpha}\left\{\frac{1}{x^2}\int_0^x (u_0 - \partial_t h)\zeta \mathrm{d}\zeta\right\}. \tag{69}$$

This equation records how the (relative) bed cover comes about from the combined effects of upstream integration of sediment supply and the downstream spreading of this sediment by fractional advection.

7. Numerical Method

[34] An approximate solution for the evolution of $C(x, t)$ over time can be written in a way that avoids differentiation and provides sufficient stability to achieve numerical solution. This is achieved by integrating out equation (67)

$$\frac{1}{\Gamma(1-\alpha)}\left\{\int_0^x (x-\zeta)^{-\alpha}C(\zeta)\mathrm{d}\zeta\right\} = -x^{-2}\left(\frac{x_0^{1-\alpha}}{v_0}\right)\left(\frac{\chi W_0 x_0}{w_0 d_0}\right)\int_0^x \zeta\Delta_t h(\zeta)\mathrm{d}\zeta, \tag{70}$$

where $\Delta_t h$ is the discretization of $\partial_t h$ with time step Δt. Using the Grünwald-Letnikov discrete approximation (equation (A6)) of the fractional integration in the left-hand side of this equation, we obtain the discrete form

$$\left(\frac{\Delta x}{x_0}\right)^{1-\alpha}\sum_{k=0}^{x/\Delta x}\frac{\Gamma(1-\alpha+k)}{k!\Gamma(1-\alpha)}C[x - k\Delta x] = -x^{-2}\left(\frac{1}{v_0}\right)\left(\frac{\chi W_0 x_0}{w_0 d_0}\right)\sum_{k=0}^{n} k(\Delta x)^2\Delta_t h[k\Delta x]. \tag{71}$$

Discretization of equation (30) is more straightforward,

$$\Delta_t h(x, t) \approx f\frac{x}{x_0}\left\{\left(\frac{\eta_r \mu Q_0}{w_0}\right)\partial_x h + \left(\frac{\eta_r}{\eta_s}\right)d_0 C\right\}\Delta t. \tag{72}$$

Solution of the model is accomplished iteratively over a linear domain $0 \le x \le x_l$ divided into a series of n nodes at intervals Δx and thus located at distances $x_k = k\Delta x$ downstream. At each time step $t \rightarrow t + \Delta t$, a set of $2n$ simultaneous equations (a pair for each node $k \in [1, n]$ using equations (71) and (72)) is derived and solved to obtain successive values of dimensionless bed cover $\{C[k\Delta x, t]\}$ and bedrock elevation $\{h[k\Delta x, t]\}$. The number of terms in the equations for bed cover increases steadily across the domain (equation (71)), which makes solution an order n problem and computation very slow for large, finely resolved profiles. A more efficient means of solution is likely to be found in the future.

[35] The boundary conditions are: (1) zero sediment influx from the drainage divide (left boundary) at $x = 0$ and (2) the elevation beyond the solution domain is held at zero $h(x \geq x_l) = 0$. The initial conditions are: (1) the initial dimensionless bed cover is zero $C(x, 0) = 0$ and (2) the initial bed slope is small and constant across the domain, $-\partial_x h = \text{const}$. Numerical solution of the successive simultaneous equations was achieved in a mixed symbolic and numerical fashion using Mathematica version 6.

8. Numerical Experiment

[36] We conducted several numerical experiments to verify the theoretical conclusions reached in sections 5 and 6, and to test the finite difference scheme derived in section 7. One of these experiments is presented here (Figures 5 and 6).

8.1. Uniform Block Uplift and Evolution to Steady State

[37] The intention of this experiment was to simulate the evolution of a mountain river channel in a moderately active tectonic and climatic environment. The following parameters were chosen:

$$\begin{aligned}
\alpha &= 1/2 \\
x_0 &= 1 \times 10^3 \text{ m} \\
Q_0 &= 2 \text{ m}^3/\text{s} \\
w_0 &= 10/\sqrt{5} \text{ m} \\
d_0 &= 1/\sqrt{5} \text{ m} \\
\chi &= 1/3 \\
W_0 &= 1 \times 10^3 \text{ m} \\
v_0 &= 100 \text{ m/a} \\
u_0 &= 1 \times 10^{-3} \text{ m/a} \\
f &= 1 \times 10^{-2} \text{ years}^{-1} \\
\mu &= 5000 \text{ s/m} \\
\eta_r &= 0.1 \\
\eta_s &= 10 \\
h_0 &= 20 \text{ m} \\
x_l &= 20 \times 10^3 \text{ m} \\
n &= 100 \\
\Delta x &= x_l/n = 200 \text{ m} \\
\Delta t &= 40 \times 10^3 \text{ years}
\end{aligned}$$

[38] These numbers define a model environment with the following properties. The catchment is $x_l = 20$ km long and $\frac{W_0}{x_0} x_l = 20$ km wide (equation (28)) with a downstream fault boundary (Figure 3), which slips at a rate $u(x_l, t) = u_0 = 1$ mm/a and which imposes a 1 mm/a rock uplift rate across the whole catchment. The erosion driven by this relative change in base level is mediated by the material properties μ, η_r and η_s, and by the frequency of characteristic discharge f, which is expressed as the number of such flood days per year; here $f = 10^{-2}$ years^{-1} or 1 day of 24-hour sustained discharge $Q(x_0) = Q_0$ about every 100 years. Sediment is supplied from the hillslopes and channels across the whole catchment at a rate set by the bedrock lowering rate along the main stream (Figures 2 and 3). The fraction of sediment transported as bedload is assumed to be a constant (across the catchment and downstream in the river) at $\chi = 1/3$.

[39] At the reference catchment scale $x = x_0 = 1$ km, the characteristic flood discharge is $Q_0 = 2$ cumecs, which is assumed to have a constant hydraulic geometry with flow width $w(x_0) = w_0 = 10/\sqrt{5}$ m and flow depth $d(x_0) = d_0 = 1/\sqrt{5}$ m for the anticipated bed slope and friction (more realistic hydraulic behavior would ultimately affect the scaling properties of the solutions, albeit weakly). The nested subcatchment width at this reference scale is $W_0 = 1$ km. The drainage area at $x = x_l$ is $A_c(x_l) = 200$ km^2 and the characteristic discharge from this area is $Q(x_l) = 400$ cumecs.

[40] The initial geometry of the landscape is a linear river bed profile (see Figures 6c and 6d) with a gradient of $-\partial_x h = 0.1\%$ and an initial elevation of $h_0 = 20$ m at the drainage divide ($x = 0$); the hillslopes and tributary channels are assumed to have already equilibrated with the mainstream geometry at $t = 0$.

[41] The time-space evolution was resolved over a uniform "grid" (vector) of $n = 100$ points with spacing $\Delta x = x_l/n = 200$ m and a time step of $\Delta t = 40$ ky. steady state was approximately achieved in about 750 ky.

8.2. Results

[42] The finite difference numerical solutions confirmed the theoretical predictions and demonstrated that the model is essentially a strongly overdamped, weakly oscillatory system that evolves stably to a steady state balance between rock uplift and mixed bedrock-alluvial channel erosion. Graphs of the model variables over x and t are shown in Figures 5 and 6. The numerical solutions (solid lines) converge to the closed form, steady state solutions (dashed lines) in all cases (see Figure 4 for comparison). These results are discussed in more detail in the next section.

9. Discussion and Conclusions

[43] We have formulated a model of bedrock river incision with sediment buffering that capitalizes on the following two innovations: (1) a single rate equation to describe both bed sediment cover removal and bedrock erosion in terms of work done on the bed and (2) treatment of the heterogeneous spreading of bed sediment using a fractional advection equation (which includes simple advection as a limiting case). Fractional advection was adopted to model the broad range of transport distances that bed sediment particles probably experience on the long-term, i.e., to deal with the combined effect of stochastic variability in grain size, bed armoring, transient depositional patterns, channel hydraulic geometry, flood discharge, and boundary shear stress, that likely generates a heavy-tailed probability distribution of particle motions (heavy-tailed pdfs of flood discharge are particularly extensively documented [e.g., *Dodov and Foufoula-Georgiou*, 2004; *Gupta et al.*, 1994; *Lague et al.*, 2005; *Molnar et al.*, 2006]). In such circumstances the classical notion of flux, and of advection and dispersion, does not work, because it assumes that local computation of the particle concentration gradient suffices

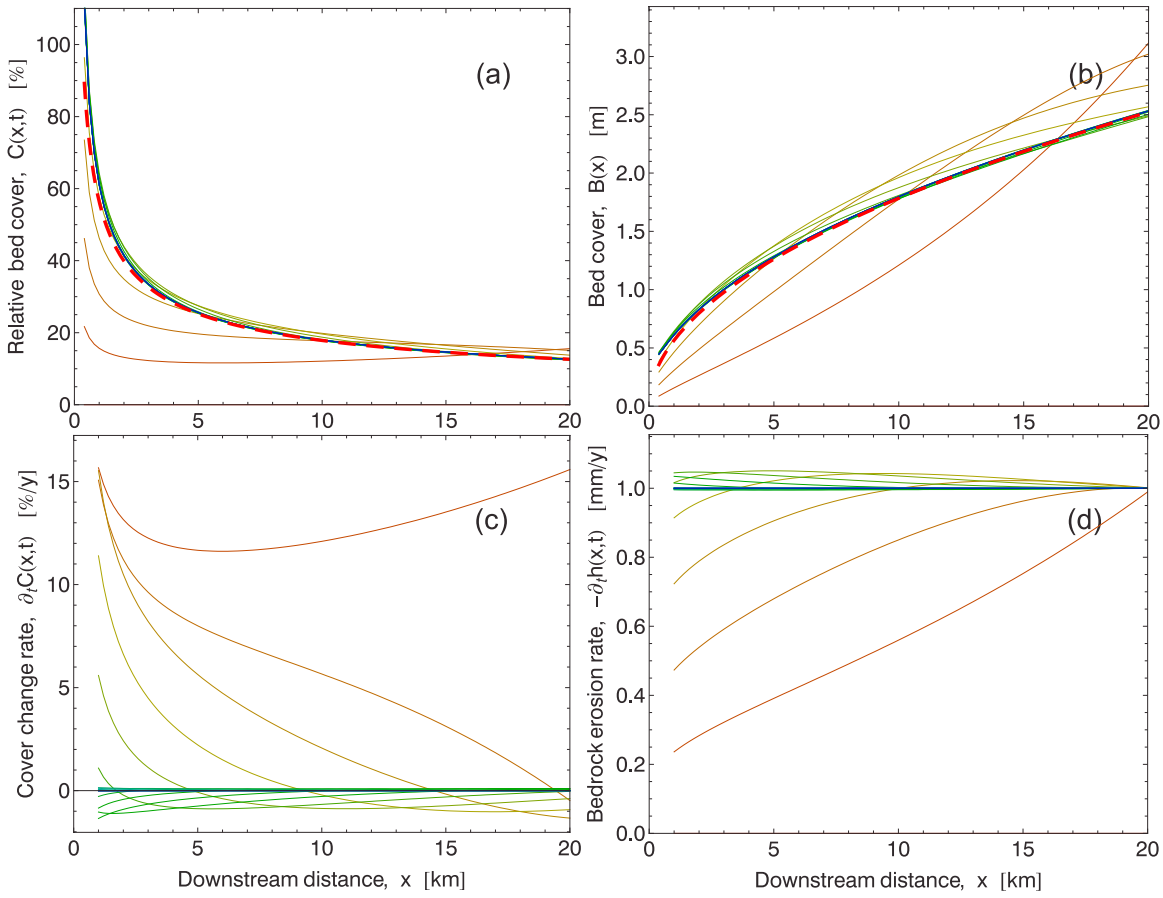

Figure 5. River profile evolution over time from an initial linear gradient to a steady state power law form obtained by numerical solution for (a) dimensionless bed cover $C(x, t)$, (b) bed cover thickness $B(x, t)$, (c) rate of change of dimensionless bed cover $\partial_t C(x, t)$, and (d) bedrock channel incision rate $-\partial_t h(x, t)$. Model parameters for this numerical simulation are given in section 8. Solid lines are numerical solutions at successive time steps; the dashed lines are the asymptotic, closed form solutions at steady state.

to estimate the numbers of particles passing by. No local computation can account for all the influxes of sediment from upstream if, on the same timescale, both short-range and long-range motions have nonvanishing probability. Instead, a nonlocal computation is needed to perform the distance-weighted sum of particle supply [*Benson*, 1998; *Cushman and Ginn*, 2000; *Berkowitz et al.*, 2002]. We have chosen fractional calculus to calculate this nonlocal flux, and we formulated a fractional advection equation that binds this nonlocal flux to the erosion of bedrock, to the buffering of the erosion rate by sediment cover, and to the hillslope-channel linked process of sediment supply.

[44] By assuming a simplified channel and catchment geometry, we have obtained closed form, steady state solutions of the two governing equations for sediment cover thickness, channel bed elevation and channel gradient as a function of downstream distance. These analytical solutions provide useful insights into the model behavior and its implications for bedrock rivers. For example, we find that if sediment buffering is very weak, a steady state logarithmic bedrock river profile is obtained (the log form originates in an assumption of simple scaling in the hydraulic geometry and in the stream power model of bedrock incision); more general scaling forms would give a power law profile. If significant buffering of bed erosion is present, nonlocal advection of sediment results in a power law profile whose scaling exponent is set by the degree of fractional advection Lévy exponent α. These results are illustrated in Figure 4 where $\alpha = 0.9$ is close to local advection and $\alpha = 0.1$ signifies a high degree of nonlocal behavior.

[45] An important model result is that at steady state the nonlocal bed sediment flux (Figure 6a) reaches a constant value all along the river (equation (48)), which is equivalent to saying that the sediment discharge per unit channel cross-sectional area, Q_s/wd, reaches a constant. Since the flux is the distance-weighted summation of mobile bed sediment upstream calculated through the fractional integral of dimensionless bed sediment $I_x^{1-\alpha}\{C(x)\}$ (equation (12)), the variable $C(x)$ must decrease downstream as a power law $C(x) \sim x^{\alpha-1}$ (equation (37)). The nonintuitive consequence is that bed sediment cover thickens more slowly than linearly downstream as $B(x) \sim x^{\alpha}$, since $0 \leq \alpha < 1$.

[46] Perhaps the most important model result is that strong sediment buffering overwhelms the scaling effect

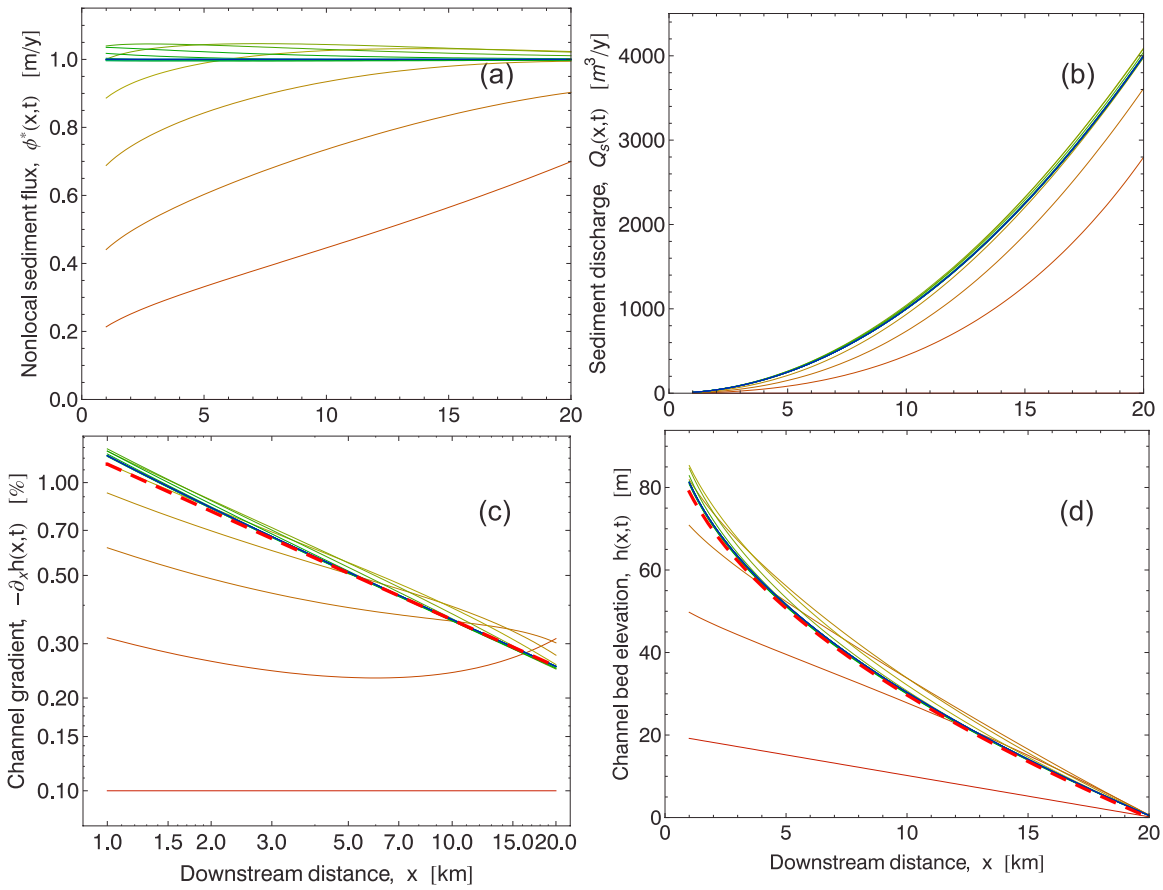

Figure 6. River profile evolution (continued from Figure 5) for (a) nonlocal bed sediment flux $\phi^*(x, t)$, (b) sediment discharge $Q_s(x, t)$, (c) bedrock channel gradient $-\partial_x h(x, t)$, and (d) bedrock channel elevation (river profile) $h(x, t)$. Solid lines are numerical solutions at successive time steps; the dashed lines are the asymptotic, closed form solutions at steady state.

of the underlying bedrock incision law [*Stark et al.*, 2000]. For heavy sediment cover, or simply at sufficient distance downstream, the asymptotic scaling of slope with upstream area is determined instead by the scaling of the fractional advection process, namely $S \sim A^{-(1-\alpha)/2}$. power law scaling of slope versus area is consistent with many empirical studies of topographic scaling [e.g., *Tarboton et al.*, 1989; *Sklar and Dietrich*, 1998; *Whipple*, 2004], for which $S \sim A^{-\theta}$ defines a "concavity index" [*Flint*, 1974] equal to $\theta = (1 - \alpha)/2$. Since typically observed values of this index are around $\theta \approx 1/2$, the empirical data are consistent with a strongly nonlocal process of sediment buffering for which $\alpha \to 0$. In fact, the simple model scaling assumptions used here (section 4) force an upper bound on our predicted concavity index of $\theta \leq 1/2$ since $\alpha \geq 0$ [*Lévy*, 1937; *Feller*, 1971; *Benson*, 1998]. However, a more general treatment of catchment and channel hydraulic scaling would relax this bound to permit higher values of $\theta > 1/2$ as observed in many analyses of digital elevation models. In any case, our model provides a radical alternative to the standard interpretation [e.g., *Montgomery*, 2001; *Whipple*, 2004] of this scaling that the concavity index is the ratio of the exponents in a stream power formulation of bedrock incision rate. A careful examination of slope-area scaling in the context of the pattern and duration of bed sediment cover in mixed bedrock-alluvial rivers may provide a means of testing these alternative models.

[47] Finally, the temporal evolution of the proposed coupled system of governing equations provides insight into the dynamics of bedrock incision. Our one-dimensional results indicate that the bedrock sediment incision interplay results in a nonlinear but highly damped system which has well behaved steady state solutions. The transient effect of powerful perturbations on this model system, particularly when extended to two dimensions (a full network), is an issue that requires further study.

Appendix A

A1. Fractional Calculus

[48] Fractional integration of order q is defined as convolution with a power law "memory" kernel, which we write as

$$I_x^q\{f\} = \frac{1}{\Gamma(q)} \int_0^x \frac{f(\zeta)}{(x-\zeta)^{1-q}} \mathrm{d}\zeta. \tag{A1}$$

The lower limit of the integral at $x = 0$ defines (in this study) the drainage divide. Fractional differentation is derived from

this convolution: in its Riemann-Liouville form the fractional derivative operator of order q is

$$\partial_x^q\{f\} = \frac{1}{\Gamma(1-q)}\frac{\mathrm{d}}{\mathrm{d}x}\left\{\int_0^x \frac{f(\zeta)}{(x-\zeta)^q}\mathrm{d}\zeta\right\} \tag{A2}$$

for $0 \leq q < 1$.

[49] Application of the fractional integral operator of order $1-\alpha$ to a power function of order β gives

$$I_x^{1-\alpha}\{x^\beta\} = \frac{\Gamma(\beta+1)}{\Gamma(\beta-\alpha)}x^{\beta-\alpha+1} \tag{A3}$$

and the fractional derivative of the same function is

$$\partial_x^{1-\alpha}\{x^\beta\} = \frac{\Gamma(\beta+1)}{\Gamma(\beta+\alpha)}x^{\beta+\alpha-1}, \tag{A4}$$

and so the fractional derivative of order $1-\alpha$ of a constant ($\beta = 0$) is

$$\partial_x^{1-\alpha}\{c\} = \frac{c}{\Gamma(\alpha)}x^{\alpha-1}. \tag{A5}$$

[50] The idea of nonlocal transport of particles can be expressed as a hopping process where the hop length belongs to a heavy-tailed probability distribution: after many hops, the Lévy limit theorem [*Lévy*, 1937; *Feller*, 1971; *Stark et al.*, 2000] predicts that the pdf of transport distance will have a Lévy stable distribution whose tail decays as a power law. The motion of particles in an aggregate sense can be expressed as a convolution of the initial spread of particles with a power law kernel with the same scaling [e.g., Cushman and Ginn 2000]. Therefore the fractional integral equation (A1) is a macroscopic description of a nonlocal hopping process. Further details can be found in, for example, *Benson* [1998], *Benson et al.* [2000a, 2000b], *Feller* [1971], *Gorenflo and Mainardi* [1997, 1999, 1998b, 1998a], *Gorenflo* [1997], *Gorenflo et al.* [1999], *Mainardi et al.* [1998], *Lévy* [1937], *Mantegna* [1994], *Meerschaert et al.* [1999], *Miller and Ross* [1993], *Oldham and Spanier* [1974], *Podlubny* [1999], *Saichev and Zaslavsky* [1997], *Samko et al.* [1993], *Samorodnitsky and Taqqu* [1994]. If the power law tail is truncated, the formalism of continuous time random walks (CTRW) is more applicable [e.g., *Berkowitz et al.*, 2002; *Mantegna and Stanley*, 1994].

[51] The Grünwald-Letnikov discrete approximation of the fractional integral operator is [*Grünwald*, 1867; *Podlubny*, 1999]

$$I_x^\gamma\{f\} = \lim_{\Delta x\to 0}(\Delta x)^\gamma \sum_{k=0}^{x/\Delta x}\frac{\Gamma(\gamma+k)}{k!\Gamma(\gamma)}f(x-k\Delta x). \tag{A6}$$

A2. Power Law Pdfs Via Mixing Distributions

[52] A common approach to treating distributions of empirical data is to assume the quantity in question belongs to a single pdf of parametric form, reducing the task to finding this form and inferring its parameters. In reality, physical data typically involve quantities derived from several "parent" quantities that are themselves distributed; even if the parent random variables belong to pdfs of classical form, the derived random variable likely will not. It is therefore safe to assume that most natural data are the result of the transformation and mixing of multiple random variables.

[53] Mixing can easily give rise to a power law pdf. For example, if one assumes that the distribution of sediment transport distances for a given grain size D is exponential then one can write

$$\mathbb{P}(X \geq x \,|\, D) = \exp(-x/\lambda_D). \tag{A7}$$

The mean transport distance is the coefficient λ_D which we assume is inversely proportional to grain size [*Hassan and Church*, 1991],

$$\lambda_D = \kappa/D. \tag{A8}$$

We further assume a gamma distribution of grain sizes

$$f(D\,|\,\alpha, D_\mathrm{m}) = \frac{\alpha^\alpha}{\Gamma(\alpha){D_\mathrm{m}}^\alpha}D^{\alpha-1}\exp\left(-\alpha\frac{D}{D_\mathrm{m}}\right), \tag{A9}$$

whose mean (not median) is D_m and whose shape parameter is $\alpha \geq 0$. Combining these equations we obtain the transport distance distribution of a grain of arbitrary (randomly selected) size

$$\mathbb{P}(X \geq x) = \left(1 + \left(\frac{D_\mathrm{m}}{\alpha\kappa}\right)x\right)^{-\alpha}, \tag{A10}$$

which is a generalized Pareto distribution. For larger hop distances $x \gg \alpha\kappa/D_\mathrm{m}$ the transport probability decays as a power law. If the duration and intensity of transport events are single valued, the distribution of particle velocities will asymptotically be as given in equation (10). If event duration and intensity (bed shear stress) are stochastic variables, further mixing will occur and the power law tail will change shape further. Summation of multiple hops will drive the long-term distribution toward a Lévy stable law with $0 \leq \alpha \leq 2$.

A3. Connection to FADE Models

[54] The nonlocal flux equation (12) is a form of fractional advection that differs from the fractional advection-dispersion equations (FADE) tailored to treat contaminant transport problems in porous media [e.g., *Benson*, 1998; *Benson et al.*, 2000a, 2000b]. In such FADE models, a fractional derivative operator is used in the dispersion term only, i.e., such models describe fractional dispersion driven by classical advection. The sole published FADE model that considers nonlocality in both the advection and dispersion terms is that of *Baeumer et al.* [2001]. Their model considers the classical advection-dispersion equation to hold locally for each particle, but at rates that vary broadly as the particle samples (during the history of its motion) more

and more of the heterogeneities of the porous medium. This formulation leads *Baeumer et al.* [2001] to consider model time as a random variable (''operational time'') and to extend the standard ADE to a combined fractional advection and fractional dispersion (FAFD) model through a stochastic operation known as subordination.

[55] The fractional advection component of the model presented here can be considered a special case of the FAFD model of *Baeumer et al.* [2001] in which, for the purpose of clarity, the dispersion term is set to zero. In the future, our model could be extended to include either classical or fractional dispersion, but the scaling effect on sediment buffering is likely to be very similar to that of the fractional advection already included in the model.

Notation

Model Variables

- t time (years).
- x distance downstream from divide (m).
- $Q(x)$ characteristic discharge (m^3/s).
- $w(x)$ flow width at characteristic discharge (m).
- $d(x)$ flow depth at characteristic discharge (m).
- $W(x)$ catchment width (m).
- $A_c(x)$ catchment area (m^2).
- $h(x, t)$ elevation of bedrock channel profile (m).
- $\Omega(Q)$ unit stream power (W/m).
- $\xi_a(x, t)$ sediment-buffered bedrock erosion rate (m/a).
- $-\partial_t h(x, t)$ rate of bed lowering (m/a).
- $-\partial_x h(x, t)$ downstream bed and energy slope (dimensionless).
- $B(x, t)$ bed sediment cover thickness (m).
- $C(x, t)$ relative bed cover (dimensionless).
- $A_s(x)$ bed sediment cross-sectional area (m^2).
- $\varphi(x, t)$ sediment supply by hillslope erosion (m^2/a).
- $\phi^*(x, t)$ downstream bed sediment flux (m/a).
- $Q_s(x)$ annual bed sediment discharge (m^3/a).
- $u(x, t)$ uplift rate pattern (m/a).

Model Parameters

- α bed cover fractional advection exponent (dimensionless).
- x_0 reference downstream distance (m).
- Q_0 characteristic water discharge at x_0 (m^3/s).
- w_0 channel flow width at x_0, Q_0 (m).
- d_0 channel flow depth at x_0, Q_0 (m).
- W_0 catchment width at x_0 (m).
- χ coarse (bed) fraction of sediment supply (dimensionless).
- v_0 reference annual bedload speed (m/a).
- u_0 uplift rate (regionally uniform) (m/a).
- f annual frequency of Q_0 flows (1/a).
- ρ density of water (kg/m^3).
- g acceleration due to gravity (m/s^2).
- γ reference erodibility (m^3/J).
- t_f duration of Q_0 flood event (s).
- μ flood effectiveness (s/m).
- $\eta_r = \eta_{rock}$ bedrock erodibility (dimensionless).
- $\eta_s = \eta_{sed}$ bed sediment erodibility (dimensionless).
- h_0 initial bed elevation at divide $x = 0$ (m).
- x_l downstream limit distance (fault boundary) (m).
- n number of resolved points along profile (dimensionless).
- Δx point spacing along profile (m).
- Δt numerical solution time step (years).
- θ slope-area scaling exponent (dimensionless).

[56] **Acknowledgments.** This work was supported by an NSF collaborative grant to Stark and Foufoula-Georgiou, EAR-0824084. It was also partially supported through grants to Stark (NASA-SENH-01 award NAG-5-13772 and NSF-GLD awards SGER EAR 05-50087 and EAR 06-17557) and to Foufoula-Georgiou (NSF Science and Technology Center, National Center for Earth-surface Dynamics (NCED) funded under contract EAR-0120914, NASA-GPM award NNX07AD33G, and funds from the Joseph T. and Rose S. Ling Professorship). This work precipitated from discussions at the working group ''Stochastic Transport and Emergent Scaling on Earth's Surface (STRESS),'' sponsored by NCED and the NSF-funded University of Illinois Hydrologic Synthesis Activity, which met in November 2007 at Lake Tahoe. The authors would like to acknowledge constructive reviews from Mark Meerschaert, Alex Densmore, and Ellen Wohl and vigorous discussions with Bill Dietrich, all of which helped significantly to improve the manuscript.

References

Baeumer, B., D. A. Benson, M. M. Meerschaert, and S. W. Wheatcraft (2001), Subordinated advection-dispersion equation for contaminant transport, *Water Resour. Res.*, *37*(6), 1543–1550.

Benson, D. A. (1998), The fractional advection-dispersion equation: Development and application, Ph.D. thesis, University of Nevada, Reno, Nev.

Benson, D. A., S. W. Wheatcraft, and M. M. Meerschaert (2000a), Application of a fractional advection-dispersion equation, *Water Resour. Res.*, *36*(6), 1403–1412.

Benson, D. A., S. W. Wheatcraft, and M. M. Meerschaert (2000b), The fractional-order governing equation of Lévy motion, *Water Resour. Res.*, *36*(6), 1413–1423.

Berkowitz, B., J. Klafter, R. Metzler, and H. Scher (2002), Physical pictures of transport in heterogeneous media: Advection-dispersion, random-walk, and fractional derivative formulations, *Water Resour. Res.*, *38*(10), 1191, doi:10.1029/2001WR001030.

Church, M., and M. A. Hassan (1992), Size and distance of travel of unconstrained clasts on a streambed, *Water Resour. Res.*, *28*(1), 299–303.

Cushman, J., and T. Ginn (2000), Fractional advection-dispersion equation: A classical mass balance with convolution-fickian flux, *Water Resour. Res.*, *36*(12), 3763–3766.

Dadson, S. J. (2004), Erosion of an active mountain belt, Ph.D. thesis, University of Cambridge, Cambridge, U. K.

Dadson, S. J., et al. (2004), Earthquake-triggered increase in sediment delivery from an active mountain belt, *Geology*, *32*(8), 733–736.

Dietrich, W. E., D. G. Bellugi, L. S. Sklar, J. D. Stock, A. M. Heimsath, and J. J. Roering (2003), Geomorphic transport laws for predicting landscape form and dynamics, in *Prediction in Geomorphology*, *Geophys. Monogr. Ser.*, vol. 135, edited by P. R. Wilcock and R. M. Iverson, pp. 103–132, AGU, Washington, D. C.

Dodov, B., and E. Foufoula-Georgiou (2004), Generalized hydraulic geometry: Derivation based on multiscaling formalism, *Water Resour. Res.*, *40*, W06302, doi:10.1029/2003WR002082.

Feller, W. (1971), *An Introduction to Probability Theory and Its Applications*, vol. 2, 2nd ed., Wiley, New York.

Finnegan, N. J., L. S. Sklar, and T. K. Fuller (2007), Interplay of sediment supply, river incision, and channel morphology revealed by the transient evolution of an experimental bedrock channel, *J. Geophys. Res.*, *112*, F03S11, doi:10.1029/2006JF000569.

Flint, J. J. (1974), Stream gradient as a function of order, magnitude, and discharge, *Water Resour. Res.*, *10*, 969–973.

Gabet, E. J., D. W. Burbank, B. Pratt-Sitaula, J. Putkonen, and B. Bookhagen (2008), Modern erosion rates in the High Himalayas of Nepal, *Earth Planet. Sci. Lett.*, *267*(3–4), 482–494.

Gorenflo, R. (1997), Fractional calculus: Some numerical methods, in *Fractals and Fractional Calculus in Continuum Mechanics*, edited by A. Carpinteri and F. Mainardi, pp. 277–290, Springer-Verlag, Wien, Germany.

Gorenflo, R., and F. Mainardi (1997), Fractional calculus: Integral and differential equations of fractional order, in *Fractals and Fractional Calculus in Continuum Mechanics*, edited by A. Carpinteri and F. Mainardi, pp. 223–276, Springer-Verlag, Wien, Germany.

Gorenflo, R., and F. Mainardi (1998a), Feller fractional diffusion and Lévy stable motions, paper presented at 5th Conference on Lévy processes: Theory and Applications, MaPhySto Cent., Dept. of Appl. Math. and Stat., Univ. of Aarhus, Copenhagen.

Gorenflo, R., and F. Mainardi (1998b), Random walk models for space-fractional diffusion processes, *Fractional Calculus Appl. Anal.*, *1*(2), 167–191.

Gorenflo, R., and F. Mainardi (1999), Approximation of Lévy-Feller diffusion by random walk, *J. Anal. Appl.*, *18*(2), 231–246.

Gorenflo, R., G. D. Fabritiis, and F. Mainardi (1999), Discrete random walk models for symmetric Lévy-Feller diffusion processes, *Physica A*, *269*, 79–89.

Grünwald, A. K. (1867), Uber "begrenzte" derivation und deren anwendung, *Z. Angew. Math. Phys.*, *12*, 441–480.

Gupta, V. K., and E. Waymire (1989), Statistical self-similarity in river networks parameterized by elevation, *Water Resour. Res.*, *25*(3), 463–476.

Gupta, V. K., O. J. Mesa, and D. Dawdy (1994), Multiscaling theory of floods: Regional quantile analysis, *Water Resour. Res.*, *30*, 3405–3421.

Harp, E. L., and R. W. Jibson (1996), Landslides triggered by the 1994 Northridge, California, earthquake, *Bull. Seismol. Soc. Am.*, *86*, S319–S332.

Hassan, M. A., and M. Church (1991), Distance of movement of coarse particles in gravel bed streams, *Water Resour. Res.*, *27*(4), 503–511.

Lague, D., N. Hovius, and P. Davy (2005), Discharge, discharge variability, and the bedrock channel profile, *J. Geophys. Res.*, *110*, F04006, doi:10.1029/2004JF000259.

Lévy, P. (1937), *Théorie de l'Addition des Variables Aléatoires*, Gauthier-Villars, Paris.

Lin, C. W., C. L. Shieh, B. D. Yuan, Y.-C. Shieh, S. H. Liu, and S. Y. Lee (2003), Impact of the Chi-Chi earthquake on the occurrence of landslides and debris flows: Example from the Chenyulan River watershed, *Eng. Geol.*, *71*, 49–61.

Mainardi, F., P. Paradisi, and R. Gorenflo (1998), Probability distributions generated by fractional diffusion equations, in *Econophysics*, edited by J. Kertèsz and I. Kondor, Kluwer, Dordrecht, Netherlands.

Mantegna, R. N. (1994), Fast, accurate algorithm for numerical simulations of Lévy stable stochastic processes, *Phys. Rev. E*, *49*, 4677–4683.

Mantegna, R. N., and H. E. Stanley (1994), Stochastic process with ultra-slow convergence to a Gaussian: The truncated Lévy flight, *Phys. Rev. Lett.*, *73*, 2946–2949.

Meerschaert, M. M., D. A. Benson, and B. Baeumer (1999), Multidimensional advection and fractional dispersion, *Phys. Rev. E*, *59*(5), 5026–5028.

Miller, K. S., and B. Ross (1993), *An Introduction to the Fractional Calculus and Fractional Differential Equations*, Wiley, New York.

Molnar, P., R. S. Anderson, G. Kier, and J. Rose (2006), Relationships among probability distributions of stream discharges in floods, climate, bed load transport, and river incision, *J. Geophys. Res.*, *111*, F02001, doi:10.1029/2005JF000310.

Montgomery, D. R. (2001), Slope distributions, threshold hillslopes, and steady-state topography, *Am. J. Sci.*, *301*, 423–454.

Oldham, K. B., and J. Spanier (1974), *The Fractional Calculus*, Academic, New York.

Podlubny, I. (1999), *Fractional Differential Equations*, vol. 198, Academic, San Diego.

Rhoads, B. (1987), Stream power terminology, *Prof. Geogr.*, *39*(2), 189–195.

Saichev, A. I., and G. M. Zaslavsky (1997), Fractional kinetic equations: Solutions and applications, *Chaos*, *7*(4), 753–764.

Samko, S. G., A. A. Kilbas, and O. I. Marichev (1993), *Fractional Integrals and Derivatives: Theory and Applications* (translated from Russian), Gordon and Breach, Zurich.

Samorodnitsky, G., and M. S. Taqqu (1994), *Stable Non-Gaussian Random Processes: Stochastic Models with Infinite Variance*, Chapman and Hall, London.

Sklar, L., and W. E. Dietrich (1998), River longitudinal profiles and bedrock incision models: Stream power and the influence of sediment supply, in *Rivers Over Rock: Fluvial Processes in Bedrock Channels*, *Geophys. Monogr. Ser.*, vol. 107, edited by K. J. Tinkler and E. E. Wohl, pp. 237–260, AGU, Washington, D. C.

Sklar, L., and W. E. Dietrich (2001), Sediment and rock strength controls on river incision into bedrock, *Geology*, *29*, 1087–1090, doi:10.1130/0091-7613(2001)029<1087:SARSCO>2.0.CO;2.

Sklar, L., and W. E. Dietrich (2004), A mechanistic model for river incision into bedrock by saltating bedload, *Water Resour. Res.*, *40*, W06301, doi:10.1029/2003WR002496.

Sklar, L., and W. E. Dietrich (2006), The role of sediment in controlling steady-state bedrock channel slope: Implications of the saltation-abrasion incision model, *Geomorphology*, *1–2*, 58–83.

Snyder, N. P., K. X. Whipple, G. E. Tucker, and D. M. Merritts (2003), Importance of a stochastic distribution of floods and erosion thresholds in the bedrock river incision problem, *J. Geophys. Res.*, *108*(B2), 2117, doi:10.1029/2001JB001655.

Stark, C. P. (2006), A self-regulating model of bedrock river channel geometry, *Geophys. Res. Lett.*, *32*, L04402, doi:10.1029/2005GL023193.

Stark, C. P., J. K. Weissel, and P. S. Dodds (2000), A Lévy diffusion model of sediment transport and landscape evolution, *EOS, Trans. AGU*, *81*(48), Fall Meet. Suppl., Abstract H12B-13.

Stock, J. D., and D. R. Montgomery (1999), Geologic constraints on bedrock river incision using the stream power law, *J. Geophys. Res.*, *104*(B3), 4893–4993.

Tarboton, D. G., R. L. Bras, and I. Rodriguez-Iturbe (1989), Scaling and elevation in river networks, *Water Resour. Res.*, *25*(9), 2037–2051.

Tinkler, K. J., and E. E. Wohl (Eds.) (1998), *Rivers Over Rock: Fluvial Processes in Bedrock Channels*, *Geophys. Monogr. Ser.*, vol. 107, AGU, Washington, D. C.

Tucker, G. E., and R. L. Bras (2000), A stochastic approach to modeling the role of rainfall variability in drainage basin evolution, *Water Resour. Res.*, *36*(7), 1953–1964.

Turowski, J. M., N. Hovius, A. Wilson, and M.-J. Horng (2008), Hydraulic geometry, river sediment and the definition of bedrock channels, *Geomorphology*, *99*(1–4), 26–38, doi:10.1016/j.geomorph.2007.10.001.

Whipple, K. X. (2004), Bedrock rivers and the geomorphology of active orogens, *Annu. Rev. Earth Planet. Sci.*, *32*, 151–185.

Whipple, K. X., and G. E. Tucker (1999), Dynamics of the stream-power river incision model: Implications for height limits of mountain ranges, landscape response timescales, and research needs, *J. Geophys. Res.*, *104*, 17,661–17,674.

Wobus, C. W., G. E. Tucker, and R. S. Anderson (2006), Self-formed bedrock channels, *Geophys. Res. Lett.*, *33*, L18408, doi:10.1029/2006GL027182, 1–6.

Zhang, Y., D. A. Benson, M. M. Meerschaert, and E. M. LaBolle (2007), Space-fractional advection-dispersion equations with variable parameters: Diverse formulas, numerical solutions, and application to the Macro-dispersion Experiment site data, *Water Resour. Res.*, *43*, W05439, doi:10.1029/2006WR004912.

E. Foufoula-Georgiou and V. Ganti, St. Anthony Falls Laboratory, University of Minnesota, 2 Third Avenue SE, Minneapolis, MN 55414, USA.

C. P. Stark, Lamont-Doherty Earth Observatory of Columbia University, 61 Route 9W, Palisades, NY 10964, USA. (cstark@ldeo.columbia.edu)